

# The Syntaxin 5 Isoforms Syx5 and Syx5L have Distinct Effects on the Processing of $\beta$ -amyloid Precursor Protein

Kei Suga<sup>1,\*</sup>, Ayako Saito<sup>1</sup>, Takami Tomiyama<sup>2</sup>, Hiroshi Mori<sup>2</sup> and Kimio Akagawa<sup>1</sup>

<sup>1</sup>Department of Cell Physiology, Kyorin University School of Medicine, Mitaka, Tokyo 181-8611; and

<sup>2</sup>Department of Neuroscience, Osaka City University Graduate School of Medicine, Osaka 545-8585, Japan

Received July 26, 2009; accepted August 20, 2009; published online August 30, 2009

**In this study, we examined the interaction of Syntaxin 5L (Syx5L), a Syx5 isoform that has an N-terminal extension containing a di-arginine ER-retrieval motif, with presenilin (PS) and its effects on the processing of  $\beta$ -amyloid precursor protein ( $\beta$ APP). Similar to Syx5, Syx5L bound to PS1 holoprotein but not to its N- or C-terminal fragments. Unlike Syx5, Syx5L overexpression did not cause marked accumulation of intracellular  $\beta$ APP holoprotein, and did not inhibit amyloid  $\beta$  peptide ( $A\beta$ ) secretion. Analyses using deletion mutants of Syx5L revealed that, in addition to the difference in the intracellular localization between the isoforms, the presence of the N-terminal extension in Syx5L was critical for suppressing its inhibition of  $\beta$ APP processing. Treatment of cells that overexpressed Syx5L with brefeldin A, an inhibitor of transport from the ER to the Golgi compartments, resulted in substantial accumulation of intracellular  $\beta$ APP holoprotein and reduction in the secretion of  $A\beta$ . Although Syx5 and Syx5L share lengthy regions of amino acid identity, they appear to play distinct roles in modulating the metabolism and trafficking of  $\beta$ APP in the early secretory compartment.**

**Key words:**  $\beta$ APP, di-arginine ER-retrieval motif, early secretory compartment, presenilin, syntaxin.

Abbreviations:  $A\beta$ , amyloid  $\beta$  peptide; AD, Alzheimer's disease; APP-CTF, C-terminal fragment of  $\beta$ -amyloid precursor protein; BFA, brefeldin A;  $\beta$ APP,  $\beta$ -amyloid precursor protein; DAPT, *N*-[*N*-(3,5-difluorophenacetyl)-*L*-alanyl]-*S*-phenylglycine *t*-butyl ester; DMEM, Dulbecco's modified Eagle's medium; ER, endoplasmic reticulum; ERGIC/VTC, ER-Golgi-intermediate compartment; HA, hemagglutinin; PS, presenilin; Syx5, syntaxin 5; SNARE, soluble N-ethylmaleimide-sensitive factor attachment protein receptor.

Many isoforms of the mammalian syntaxin (Syx) family localize to specific membrane compartments along the secretory and endocytotic pathways and are thought to act as soluble *N*-ethylmaleimide-sensitive factor-attachment protein receptors (SNAREs) in intracellular vesicle trafficking (1–3). Among Syx family proteins, Syx5 is found primarily in the endoplasmic reticulum (ER) through the Golgi compartments in the early secretory pathways, and in the post-*trans* Golgi network/endocytotic pathways (4, 5). Syx5 is thought to regulate the potential targeting and fusion of carrier vesicles at multiple membrane fusion interfaces by affecting the selective combination of the SNARE complex with other SNARE-related proteins (6–9). Mammalian Syx5 is unique in having two isoforms that are generated from alternative translation initiation sites on the same messenger RNA (10). Relative to the 35-kDa isoform (designated Syx5), the 42-kDa isoform (designated Syx5L) has an extended N-terminal region, which contains a type-II di-arginine ER retrieval motif (7, 10, 11). However, whether the two Syx5 isoforms have distinct functional roles remains unknown.

Presenilin (PS) and  $\beta$ -amyloid precursor protein ( $\beta$ APP) are the key players in the production of amyloid  $\beta$  peptide ( $A\beta$ ), which is implicated in the pathogenesis of Alzheimer disease (AD) (12). PS1 is closely linked to the processing of  $\beta$ APP into the  $A\beta$  peptides  $A\beta$ 40 and  $A\beta$ 42 and has been widely accepted to be the catalytic component of  $\gamma$ -secretase (13). PS co-factors, such as nicastrin, APH1, and PEN-2, have been shown to form a complex with PS and play a role in coordination of the catalytic activity of the PS/ $\gamma$ -secretase complex (13). Recent studies have demonstrated that  $\gamma$ -secretase biogenesis, complex formation and  $\beta$ APP processing occur in the early secretory compartments (14–16). However, the determinants of PS progression along the secretory pathways and the mechanisms of intracellular trafficking of  $\beta$ APP remain poorly understood.

We previously showed that Syx5, a SNARE protein of the early secretory compartment, specifically interacts with PS holoproteins, but not with the N- or C-terminal fragments of PS (17, 18). We also mapped the interaction domains of Syx5 to its cytoplasmic and transmembrane regions. Syx5 overexpression was shown to up-regulate  $\beta$ APP accumulation in the ER through the Golgi compartments, attenuate accumulation of the C-terminal fragment of  $\beta$ APP (APP-CTF), and reduce  $A\beta$  secretion (17, 18). Except for the N-terminal extension domain of Syx5L, the overall structures of Syx5 and Syx5L are well

\*To whom correspondence should be addressed.  
Tel: +81-0422-47-5511, Fax: +81-0422-47-4801,  
E-mail: ksuga@ks.kyorin-u.ac.jp

conserved, suggesting that similar to Syx5, Syx5L might interact with PS and regulate the processing or trafficking of AD-related proteins. Therefore, in the present study, we examined whether Syx5L, which is relatively highly expressed in neuronal cells compared to Syx5 (19), has similar effects to Syx5. We found that Syx5L also binds to PS holoproteins in the ER and Golgi compartments. However, the two Syx5 isoforms exhibited disparate behaviors in modulating the metabolism and trafficking of  $\beta$ APP in the early secretory compartment.

## MATERIALS AND METHODS

**Materials and Antibodies**—Mouse  $\alpha$ PS1 antibody (PSN2) recognizes N-terminal residues 31–56 of PS1. Rabbit polyclonal antibodies  $\alpha$ S182Nterm2nd ( $\alpha$ PS1N) and AD3loop3rd ( $\alpha$ PS1C) recognize the N- and C-terminal fragments, respectively. The rabbit polyclonal antibody to  $\beta$ APP (C40) recognizes the last 40 amino acid residues in the C-terminus of human  $\beta$ APP (18). The rat monoclonal anti-hemagglutinin (HA) antibody 3F10 and anti-c-Myc antibody 9E10 were purchased from Roche Diagnostics (Indianapolis, IN, USA). Mouse monoclonal antibodies against GM130, calnexin, and  $\gamma$ -adaptin were obtained from BD Transduction Laboratories (San Diego, CA, USA). Mouse monoclonal antibody against  $\alpha$ -tubulin was purchased from Sigma (St Louis, MO, USA). The polyclonal rabbit anti- $\beta$ COP antibody and mouse monoclonal antibody to sarco/endoplasmic reticulum  $\text{Ca}^{2+}$ -ATPase 2 (SERCA2) were obtained from Affinity Bioreagents (Golden, CO, USA). Alexa Fluor 488 anti-mouse, anti-rat, and anti-rabbit IgGs were purchased from Molecular Probes (Eugene, OR, USA). Cy3-labelled anti-rat and anti-mouse IgGs were purchased from Jackson Immunoresearch Laboratories (West Grove, PA, USA). Rhodamine-labelled anti-rabbit IgG was purchased from Cappel (Aurora, OH, USA). Hoechst 33342 and brefeldin A (BFA) were purchased from Sigma. BFA was stored in 5 mg/ml methanol solution. *N*-[*N*-(3,5-difluorophenacetyl)-*L*-alanyl]-*S*-phenylglycine *t*-butyl ester (DAPT) was purchased from Calbiochem (San Diego, CA, USA) and was prepared by dissolution in dimethyl sulfoxide. Protease inhibitor cocktail was purchased from Wako Chemicals (Osaka, Japan). All other reagents were of the highest grade available, unless otherwise noted.

**Plasmid Construction**—Expression plasmids for the cDNAs encoding HA-tagged full-length human Syx5 (h5-pcDNA3HAN) and Syx5L (h5L-pcDNA3HAN) were described previously (17–19). The cDNA fragments encoding full-length Syx5 and Syx5L were produced by PCR using a 5'-primer containing an additional in-frame *Bam*HI site and the 3'-SP6 primer present in the pcDNA3 vector. After digestion with *Bam*HI and *Xba*I, the PCR products were inserted into the *Bam*HI–*Xba*I site of the pcDNA3-myc vector in frame to produce the plasmids Myc-h5-pcDNA3 and Myc-h5L-pcDNA3, respectively. N-terminal deletion mutants of Syx5L (HA-Syx5L $\Delta$ 1–6 and HA-Syx5L $\Delta$ 1–30) were constructed by inserting PCR fragments digested with *Bam*HI and *Xho*I into the *Bam*HI–*Xho*I site of the pcDNA3-HAN vector. The Syx5L-RKR-AAA (Syx5LA) mutant was

generated from the wild-type h5L plasmid using a QuikChange Site-Directed Mutagenesis kit (Stratagene, San Diego, CA, USA) with the appropriate synthetic oligonucleotides. The expression plasmids encoding the full-length human PS1 protein (PS1-pCI) and the human wild-type  $\beta$ APP695 (APP695-pCI) were described previously (17, 18). Sequences of all constructs were verified both by direct sequencing on an ABI373A Sequencer with a BigDye filter (Applied Biosystems Japan, Tokyo, Japan) and by analysis with the appropriate restriction enzymes.

**Cell Culture, Transfection and Extract Preparation**—Mouse neuroblastoma and rat glioma hybrid NG108-15 cells were cultured in a humidified incubator with 5%  $\text{CO}_2$  at 37°C in Dulbecco's modified Eagle's medium (DMEM) containing 4 mM *L*-glutamine, 100 U/ml penicillin, 100  $\mu$ g/ml streptomycin, 2.5 mM hypoxanthine, 10  $\mu$ M aminopterin, 0.4 mM thymidine and 10% fetal bovine serum (FBS), as described previously (18, 19). Cells were inoculated into Type IV-collagen coated 6-well plates (BD Bioscience, Bedford, MA, USA) for western blotting and enzyme-linked immunosorbent assay (ELISA) or into 35-mm dishes with glass bottoms for immunocytochemical analysis. Cells were transfected using FuGENE6 ( $\mu$ l) transfection reagent (Roche Diagnostics) and DNA ( $\mu$ g) in a ratio of 5:1 after replacement of the medium with fresh medium, as described previously (18, 20). After collecting the culture supernatant in each well, transfected cells were washed three times with 4 ml of phosphate-buffered saline (PBS, pH 7.4) and were harvested with a cell scraper. Cells were recovered by centrifugation at 1,500g at 4°C for 3 min, and resultant cell pellets were lysed in 150  $\mu$ l of extraction buffer [50 mM Tris–HCl (pH 7.5), 0.15 M NaCl, and 1% Triton X-100] containing a protease inhibitor cocktail and sonicated for 30 s. The insoluble material was removed by centrifugation at 15,000g for 10 min, and the supernatant fraction was used as the extract sample. After determination of the protein content by the Bradford method (21) with bovine serum albumin as a standard, Laemmli sample buffer (22) was added for use in Tris/Glycine SDS–PAGE, or SBG (Serva blue G; Serva electrophoresis, Heidelberg, Germany) sample buffer [50 mM Tris–HCl (pH 6.8), 4% SDS, 12% glycerol, 2% 2-mercaptoethanol, 0.01% SBG] was added for use in Tris/Tricine SDS–PAGE (23). After, solubilization in SDS sample buffer for 30 min at 37°C, the extracted samples were frozen and stored at –80°C until use.

**Immunoprecipitation, SDS–PAGE and Western Blotting**—A 50% slurry of Protein G-Sepharose beads (GE Biosciences, Piscataway, NJ, USA) in extraction buffer (total volume, 100  $\mu$ l) was added to cell extracts (450  $\mu$ l) prepared from each well of the 6-well plates and incubated for 1 h at 4°C. Aliquots (50  $\mu$ l) of pre-cleared lysates were collected as the 'Input' sample and the remaining 400  $\mu$ l of the lysates was further incubated with anti-PS polyclonal antibodies (1  $\mu$ l of serum) or anti-HA antibody (3F10, 0.5  $\mu$ g) for 2 h at 4°C. The immunocomplexes were then precipitated at 4°C for 4 h using 100  $\mu$ l of 50% slurry of Protein G-Sepharose beads. The beads were washed twice with 1 ml of the extraction buffer followed by a single wash with 1 ml of 50 mM

Tris-HCl (pH 7.5), and the bound proteins were eluted by incubating with 40  $\mu$ l of Laemmli sample buffer at 37°C for 30 min. The beads were removed by centrifugation at 15,000g for 3 min, and the supernatant fraction was used as the immunoprecipitated sample. The samples were subjected to SDS-PAGE and western blotting, as described previously (18, 19) with minor modifications. The extracted samples (10–40  $\mu$ g of protein/lane) were subjected to electrophoresis on Tris/Glycine 10 or 12% SDS-polyacrylamide gels according to the methods of Laemmli (22), or on Tris/Tricine 16.5% SDS-polyacrylamide, as described previously (18, 23). Proteins that had been separated in the gels were transferred onto polyvinylidene fluoride (PVDF) membranes (Immobilon P, Millipore Corp., Bedford, MA, USA) using a semi-dry blotting apparatus (Nihon eido, Tokyo, Japan) for 2 h at 4°C. The membranes were blocked with 5% skimmed milk in PBS that contained 0.1% Tween-20 (PBS-T) for 1 h at room temperature, and subsequently labeled with the primary antibody for 1.5 h. After washing in PBS-T, the blots were labelled with either affinity purified horse radish peroxidase (HRP-) conjugated or biotinylated goat-anti-mouse, -rabbit or -rat IgG (1:4,000; Vector Laboratories Inc., Burlingame, CA, USA) in PBS-T for 30 min at room temperature. Biotinylated immunocomplexes were detected using avidin-conjugated HRP (1:4000; Vector) in PBS for 30 min at room temperature. After washing with PBS-T followed by PBS, immunoreactive bands were visualized using enhanced chemiluminescence reagents (ECL; GE Healthcare Ltd., UK) and were analyzed by densitometry using an LAS3000 imaging system and MultiGauge software (FujiFilm, Tokyo, Japan). Blots were also exposed to Hyper film (ECL; GE Healthcare Ltd.).

**Discontinuous Sucrose Density Gradient Fractionation**—Discontinuous sucrose density fractionation, which enriches ER- and Golgi-derived vesicles, was performed as described previously (18, 24). Transfected NG108-15 cells were washed with PBS and harvested from 100-mm dishes using a cell scraper and recovered by centrifugation. Cells were homogenized in homogenization medium [10 mM Tris-HCl (pH 7.4), 0.25 M sucrose, 1 mM MgCl<sub>2</sub>, plus the protease inhibitor cocktail] in a final mixture of 1 volume of cell pellet to 5 volumes of homogenizing medium. The homogenate (1 ml) was loaded onto the top of a step gradient that comprised 1 ml of 2 M sucrose, 4 ml of 1.3 M sucrose, 3.5 ml of 1.16 M sucrose and 2.0 ml of 0.8 M sucrose. All of the solutions contained 10 mM Tris-HCl (pH 7.4) and 1 mM MgCl<sub>2</sub>. The gradients were centrifuged for 2.5 h at 100,000g in a Hitachi P28S2 rotor in an ultracentrifuge (Hitachi, 70P-72). Thirteen 750  $\mu$ l fractions were collected from the top of the gradient and assayed for total protein content by the method of Bradford, with BSA as the standard. SDS sample buffer (5 $\times$ ) was added to each fraction, and they were stored at -80°C until use. Twenty microlitres of each fraction was subjected to SDS-PAGE and western blotting. The heavy fractions (#4–12) were ER-enriched, as determined by the presence of calnexin, an ER marker. The light fractions (#1–4) were Golgi-enriched, as determined by the presence of

three different Golgi markers:  $\beta$ COP for the ER-Golgi intermediate compartment (ERGIC/VTC) and the Golgi apparatus,  $\gamma$ -adaptin for the *trans*-Golgi network, and GM130 for the *cis*-Golgi, as described previously (18, 24).

**Immunocytochemistry**—After 24 h of transfection, cells were fixed and stained, as described previously (18, 20). The cells were washed with PBS and fixed with 3.7% paraformaldehyde in PBS for 15 min at room temperature. After fixation, the cells were washed with PBS and permeabilized for 15 min with PBS containing 0.1% Triton X-100 and 5% normal goat serum (NGS-PBSTX). The cells were then incubated with primary antibody in NGS-PBSTX for 1.5 h at room temperature. After washing with PBSTX, the cells were incubated for 1 h at room temperature with the secondary antibody (1:1,000) in NGS-PBSTX containing 1  $\mu$ g/ml Hoechst 33342. Digital images of stained cells were acquired using an IX70 inverted microscope (Olympus) with a 60 $\times$  PlanApo lens (numerical aperture, 1.4 oil immersion) equipped with a CoolSNAP CCD camera (Roper Scientific, Trenton, NJ, USA) using appropriate filters for excitation and emission. Images were collected as TIFF files using Metamorph software (Universal Imaging Corporation, Downingtown, PA, USA) and processed using Adobe Photoshop software (Mountain View, CA, USA).

**Quantification of A $\beta$  by Sandwich ELISA**—Cells were plated on 6-well plates (in 4 ml of medium) 2 days before transfection. After the medium was replaced with fresh medium, the cells were transfected with the indicated plasmids along with cDNA encoding APP695 (APP695-pCI) in the absence or presence of 2  $\mu$ M DAPT, a  $\gamma$ -secretase inhibitor, or the presence of 0.2  $\mu$ g/ml BFA, a fungal toxin that inhibits transport from the ER to the Golgi compartments. The culture medium was collected 48 h after transfection, cell debris was removed by centrifugation at 15,000g for 3 min, and the supernatant fraction was used as the ELISA sample. A $\beta$ 40 and A $\beta$ 42 secreted into the culture medium (50 and 100  $\mu$ l, respectively) were quantified using sandwich ELISAs specific for each peptide according to the manufacturers' instructions (BioSource, Camarillo, CA, USA and Wako chemicals, Osaka, Japan, respectively).

## RESULTS

**Syx5 and Syx5L Localize Differently in NG108-15 Cells**—Two Syx5 isoforms are ubiquitously expressed in various cells, including neurons. The longer isoform Syx5L has a putative type-II di-arginine ER-retrieval motif (<sup>4</sup>RKR<sup>6</sup>) in its N-terminal extension region (Fig. 1A). To characterize the different properties of the Syx5 isoforms, we first examined the intracellular localization of the two isoforms. Intracellular localization of wild-type and mutant Syx5 isoforms that were tagged at their N-termini with either a Myc or HA epitope in NG108-15 cells were studied immunocytochemically. In Western blot analysis of cells that overexpressed Syx5L, the density of the band corresponding to Syx5 was unchanged compared to that of control cells, indicating that negligible alternative initiation of



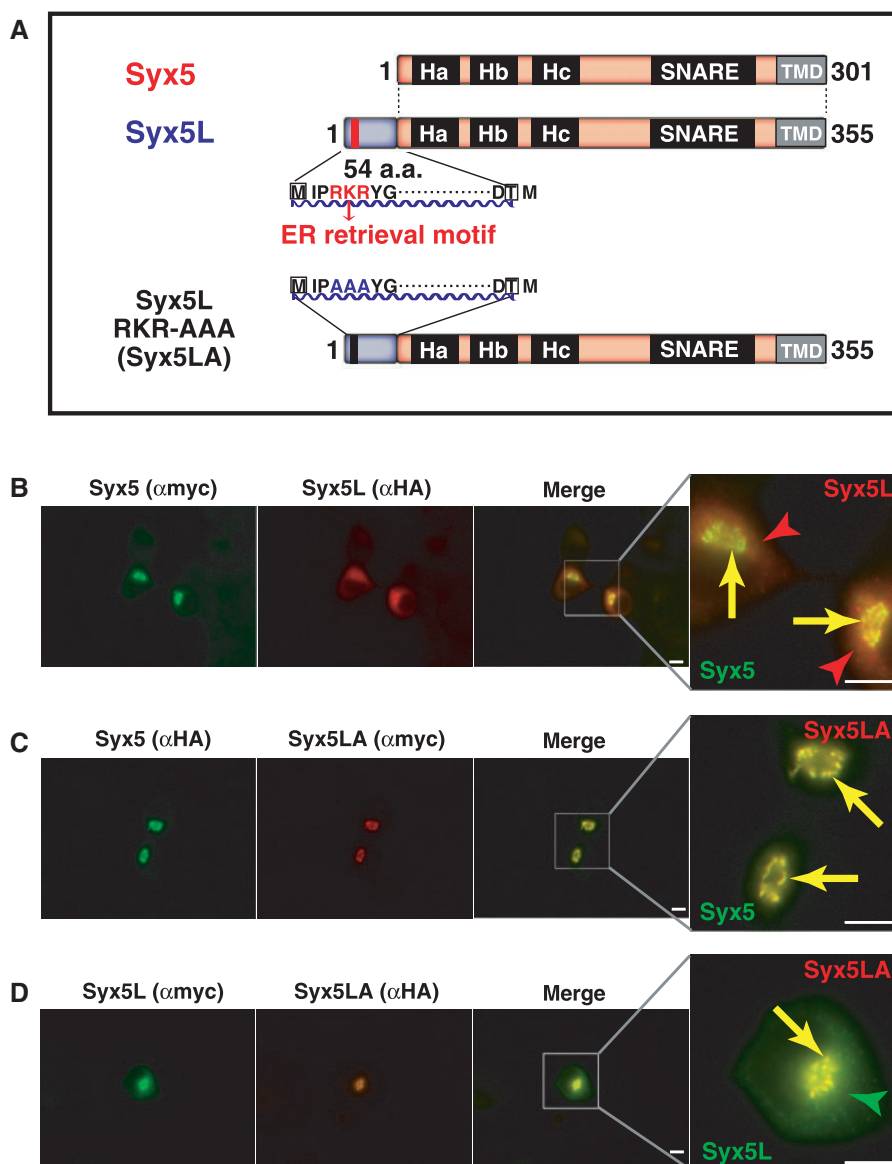


**Fig. 1. Intracellular localization of Syx5 isoforms in NG108-15 cells.** (A) Schematic domain structures of Syx5 (35 kDa), its longer isoform Syx5L (42 kDa) and the Syx5L mutant Syx5LA. The putative  $\alpha$ -helices (Ha, Hb, Hc and SNARE motif) and the transmembrane region (TMD) of the Syx5 isoforms are indicated in black and gray, respectively. The N-terminal extension domain in Syx5L is shown in blue, and partial sequences of the N-terminal extension domain in Syx5L are illustrated. The putative di-arginine ER-retrieval motif (<sup>4</sup>RKR<sup>6</sup>) is typed in red. In the Syx5LA mutant, the motif in

the N-terminal extension domain of Syx5L is replaced with alanines. (B) Double-label immunofluorescence images of NG108-15 cells co-transfected with plasmids encoding N-terminally tagged Syx5 isoforms (HA-Syx5L and Myc-Syx5). Cells were fixed 24 h after transfection and stained with monoclonal anti-HA (3F10; 1:100) and anti-Myc (9E10; 1:100) antibodies. (C and D) Myc- or HA-tagged Syx5LA mutant constructs were co-transfected into NG108-15 cells together with plasmids containing the wild-type Syx5 isoforms and stained as described in the MATERIALS AND METHODS section. Bar, 10  $\mu$ m.

translation occurred (data not shown). Double-label immunocytochemical analysis using anti-HA and anti-Myc antibodies showed that both Syx5 isoforms co-localized in the Golgi ribbon (Fig. 1B, yellow arrows), but the localization of Syx5L in the ER was prominent (Figs. 1B and D, red and green arrowheads, respectively). Studies in cells that expressed HA-tagged Syx5 or Myc-tagged Syx5L yielded similar results (data not shown). We confirmed that both isoforms were primarily distributed in the Golgi compartments, and some portion of

Syx5L was distributed in the ER (supplementary Figure S1). We also determined the intracellular localization of a Syx5L mutant lacking the ER-retrieval motif (Syx5LA, Fig. 1A). This Syx5LA mutant co-localized almost exactly with Syx5 (Figs. 1C and D, yellow arrows) in the Golgi ribbon as revealed by the presence of the Golgi marker (Supplementary Figure S1). Collectively, these results show that Syx5 and Syx5L have slightly different distributions and that the di-arginine ER retrieval motif in Syx5L is functional

in NG108-15 cells. These findings are consistent with those reported in other cell types (10).

**Syx5L Co-localizes and Interacts with PS Holoproteins in the Early Secretory Compartments of NG108-15 Cells**—We previously showed that, among the isoforms of Syx thus far examined (Syx1A, 2, 3A, 4, 5, 6, 7 and 8), Syx5 co-localized with PS in the ER and Golgi compartments, and Syx5 specifically binds to PS holoproteins with its cytoplasmic and transmembrane domains (17, 18). Because Syx5L possesses the domains of Syx5 that are responsible for its interaction with PS (Fig. 1A), we examined whether Syx5L co-localized and interacted with PS1. As shown in Fig. 2A, Syx5L co-localized primarily with PS1 in the Golgi ribbon and partially in the ER of NG108-15 cells. Sucrose density gradient (SDG) fractionation analysis was performed in order to enrich the ER- and Golgi-derived vesicles (Fig. 2B). The vesicle coat protein  $\beta$ COP co-distributed and intersected with

PS1 at the ER-Golgi junction, where Syx5 isoforms were enriched. PS1 holoprotein (PS1FL) was broadly localized throughout the ER and Golgi fractions (#4–12), where it co-localized with Syx5L; whereas the N-terminal proteolytic fragment of PS1 (PS1NTF) was distributed predominantly in the light Golgi fractions (#1–4).

We next examined whether Syx5L also interacted with PS1. As shown in Fig. 3A,  $\alpha$ HA antibody co-precipitated PS1 holoprotein (PS1FL) (asterisk in Fig. 3A), but did not precipitate the proteolytically cleaved C-terminal fragments of PS1 (PS1CTF). The N-terminal fragment of PS1 (PS1NTF) was not also co-precipitated with Syx5L in NG108-15 cells (Fig. 3B). Reverse immunoprecipitation analyses using the anti-PS1 antibody confirmed the precipitation of Syx5L with PS1 holoprotein (Fig. 3C). These results suggest that Syx5L and PS1 holoprotein are co-localized in the ER through the Golgi

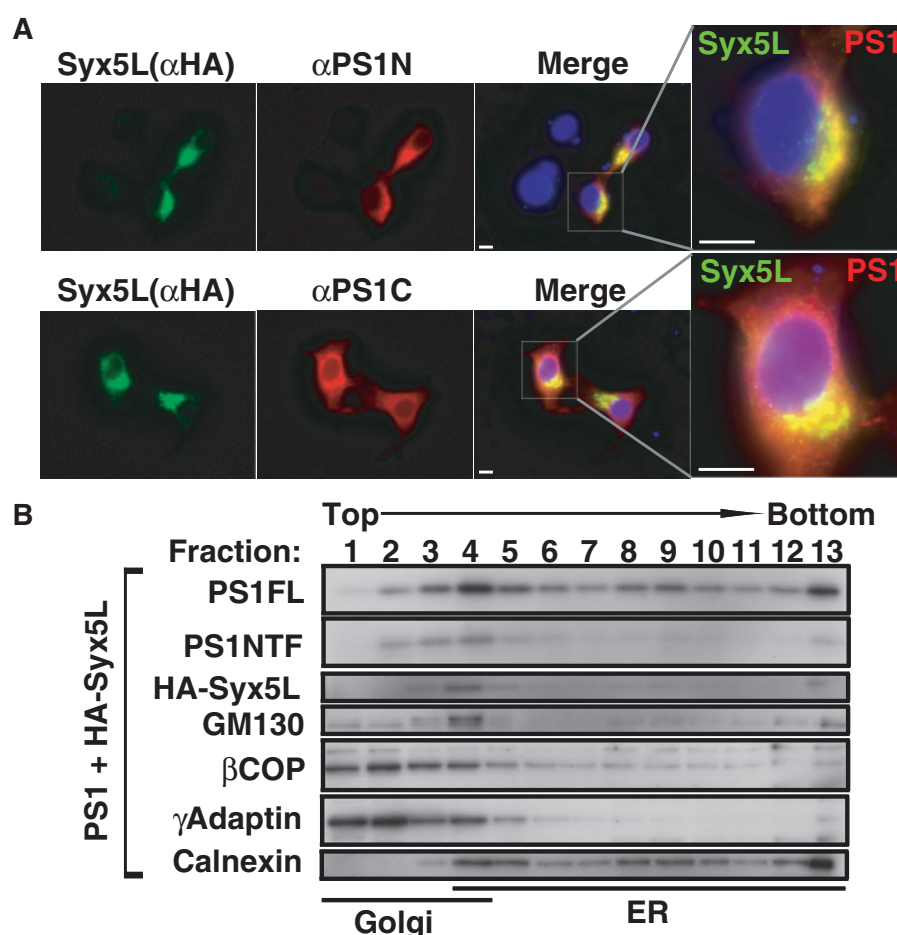


**Fig. 2. Intracellular localization of Syx5L and PS1 proteins.** (A) NG108-15 cells were co-transfected with the plasmid that expresses Syx5L (h5L-pcDNA3HAN) and the plasmid that expresses wild-type PS1 (PS1-pCI). After transfection, cells were stained with the anti-HA antibody (3F10) in combination with either the anti-PS1N-terminus polyclonal antibody ( $\alpha$ PS1N; 1:200) or the anti-PS1C-terminus polyclonal antibody ( $\alpha$ PS1C; 1:200), respectively. The cell nuclei were counterstained with Hoechst 33342 (blue). Bar, 10  $\mu$ m. (B) Homogenates from cells co-transfected with plasmids expressing PS1 and

HA-Syx5L were subjected to SDG fractionation analysis followed by SDS-PAGE and western blotting, as described in the MATERIALS AND METHODS section. The PS1 holoprotein (PS1FL) and N-terminal fragment of PS1 (PS1NTF) were probed with antibody (PSN2) that recognizes the N-terminal region of PS1. HA-Syx5L was probed with the anti-HA antibody (3F10; 1:2,000). Subcellular markers for the ER and Golgi compartments were probed with the indicated antibodies, as described in the MATERIALS AND METHODS section.

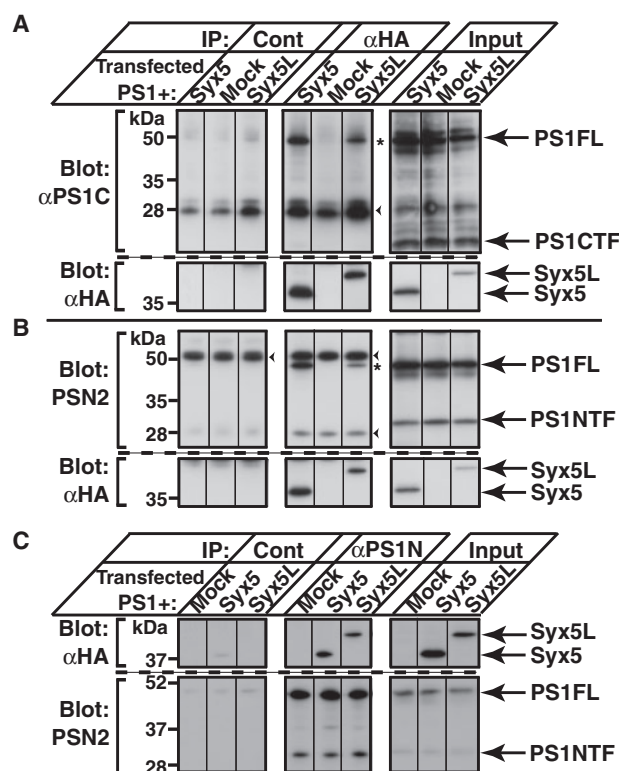


**Fig. 3. Interaction of Syx5L with full-length PS1 holoprotein.** NG108-15 cells were co-transfected with plasmids expressing PS1 and either HA-Syx5 or HA-Syx5L or the empty pcDNA3 vector (Mock). Two days after transfection, the cell extracts were immunoprecipitated, and the immunocomplexes were subjected to SDS-PAGE and western blotting, as described in the MATERIALS AND METHODS section. Representative images are shown. Immunocomplexes were precipitated with 3F10 (αHA) or normal rat IgG (Cont) and were probed with antibodies against the C- (A) and N-terminus (B) of PS1, respectively. The 'Input' panels show the PS protein bands in the 'Input' fraction that were probed with mouse polyclonal antibody against the N-terminus of PS1 (PSN2 1:4,000) or αPS1C (1:4,000). Bands corresponding to PS1 holoproteins (PS1FL) that co-precipitated with Syx5L are marked with the asterisks. Heavy and light chains of IgG are marked with arrowheads. (C) Syx5 isoforms were precipitated with rabbit polyclonal antibody to the N-terminus of PS1 (αPS1N) and were probed with antibody against HA (3F10) or the antibody against the N-terminus of PS1 (PSN2).

compartments and that, similar to Syx5, Syx5L interacts with PS1 holoprotein, but not with the N- or C-terminal PS1 fragments.

**Overexpression of Syx5L does not Inhibit the Processing of βAPP**—Because the overexpression of Syx5 up-regulated the intracellular accumulation of βAPP and down-regulated the secretion of Aβ (17, 18), we examined whether the Syx5L isoform also affected the processing of βAPP in NG108-15 cells. As the two Syx5 isoforms are presumably generated from a single messenger RNA during translation (10), it was technically impossible to selectively down-regulate each isoform by small interfering RNA methods (19). Therefore, we examined their differences in an overexpression system. Cells were co-transfected with a plasmid expressing

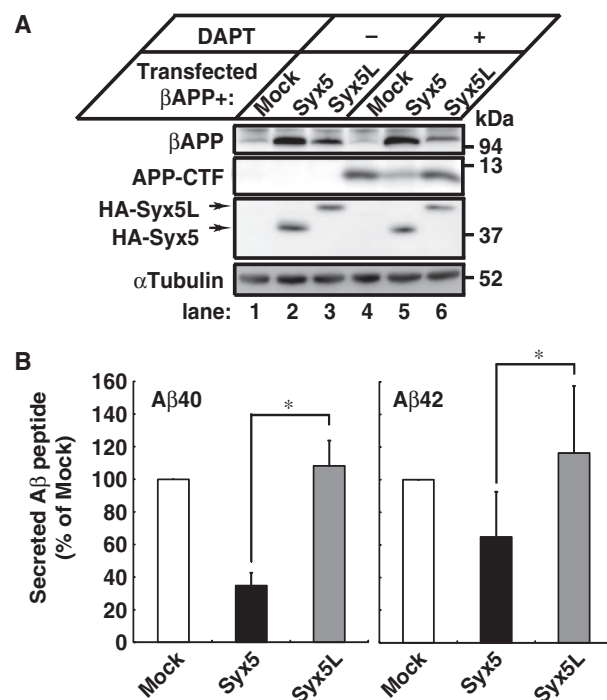


**Fig. 4. Overexpressed Syx5 isoforms have different effects on βAPP processing.** (A) NG108-15 cells were co-transfected with the indicated plasmids along with a cDNA encoding βAPP (APP695-pCI) in the absence (–, vehicle, lanes 1–3) or presence (+, 2 μM, lanes 4–6) of the γ-secretase inhibitor DAPT. Cell extracts prepared 48 h after transfection were subjected to SDS-PAGE and immunoblotted with 3F10 and anti-βAPP (C40; 1:2,000) antibodies. Comparable amounts of Syx5 isoforms were overexpressed, and an α-tubulin antibody (1:20,000) was used to verify that equal amounts of protein were loaded in each lane. A representative image is shown. (B) The amount of secreted Aβ40 and Aβ42 from the cells in the absence of DAPT was quantified by selective sandwich ELISA, as described in MATERIALS AND METHODS section and calculated as a percentage of the control (Mock). Values shown represent the mean ± SD for 18–19 independent samples. \**P* < 0.001 as determined by Student's *t*-test.

either Syx5 or Syx5L and a plasmid expressing βAPP. Significant accumulation of intracellular βAPP was observed in cells that overexpressed Syx5 (Fig. 4A, top panel, lane 2), as reported previously (18), but less accumulation was observed in cells that overexpressed Syx5L (top panel, lane 3). Because of the high γ-secretase activity in this cell line, APP-CTF in untreated cells was hard to detect; thus, we treated the cells with the γ-secretase inhibitor DAPT to determine the steady-state level of APP-CTF derived from βAPP. APP-CTF was clearly detectable in all βAPP-overexpressing cells treated with DAPT (Fig. 4A, 2nd panel, lanes 4–6), and this treatment abolished Aβ40 secretion in those cells (<5% of that in untreated cells). Although the level of APP-CTF accumulated in cells that overexpressed Syx5 was decreased (lane 5), it is noteworthy that overexpression of Syx5L did not result in a significant decrease in the level of APP-CTF (lane 6). In the absence of DAPT, the overexpression of Syx5 significantly reduced the secretion of Aβ40 and Aβ42 (Fig. 4B, black bars) ( $34.8 \pm 7.9\%$  and



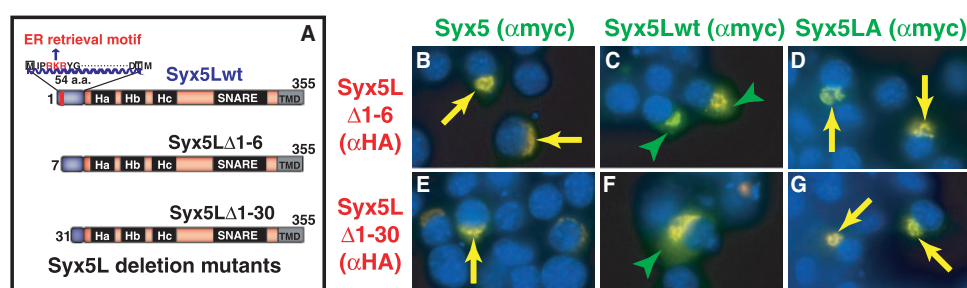


Fig. 5. **Intracellular localization of deletion mutants of Syx5L.** (A) Schematic domain structures of Syx5L deletion mutants. Six and 30 amino acids were deleted from the N-terminus (numbered from the first AUG codon of the sequence) and substituted with the HA epitope in frame to produce HA-Syx5LΔ1-6 and HA-Syx5LΔ1-30, respectively. (B–G) Double-label immunofluorescence images of NG108-15 cells

co-transfected with plasmids encoding HA-Syx5LΔ1-6 or HA-Syx5LΔ1-30 together with Myc-tagged Syx5 isoforms stained with anti-HA (3F10; 1:100) and anti-Myc (9E10; 1:100) antibodies, as described in the MATERIALS AND METHODS section. Co-localization of the two constructs expressed in the Golgi ribbon is indicated with yellow arrows. Expressed Syx5L proteins present in the ER are indicated by green arrowheads.

$64.9 \pm 27.7\%$  of that in cells co-transfected with empty plasmid [Mock], respectively,  $P < 0.001$ ), whereas the overexpression of Syx5L did not reduce the secretion of A $\beta$ 40 (gray bars) ( $108.4 \pm 15.3\%$  of Mock,  $P = 0.064$ ) and A $\beta$ 42 ( $116.4 \pm 41.2\%$  of Mock,  $P = 0.11$ ). The overexpression of Syx5, but not Syx5L, inhibited A $\beta$  secretion and increased intracellular accumulation of  $\beta$ APP.

**Effect of Syx5L Mutants on the Processing of  $\beta$ APP—**Because Syx5L has an N-terminal extension containing a functional type-II di-arginine ER retrieval motif ( $^4$ RKR $^6$ , Fig. 5A), the presence of this domain (or the motif) may clarify the difference between the isoforms. We took advantage of the Syx5LA mutant and deletion mutants of Syx5L with the HA-tag (Fig. 5A) to investigate the consequences of the difference in  $\beta$ APP processing in the intracellular localization of the two isoforms. As shown in Figure 5, double-label immunocytochemical analysis using anti-HA and anti-Myc antibodies showed that all deletion mutants so far studied (Fig. 5B–G) were almost exactly co-localized with Syx5 and the Syx5LA mutants (yellow arrows). In addition, immunocytochemical analysis using the ER and Golgi markers (Supplementary Fig. S1) showed that these deletion mutants were located mainly in the Golgi ribbon and were almost absent from the ER where some portion of wild-type Syx5L was localized (Fig. 5C and F, green arrowheads). These observations again suggest that the di-arginine ER retrieval motif in the N-terminal extension domain is necessary for Syx5L isoforms to locate in the ER.

The effect of these Syx5L mutants on the processing of  $\beta$ APP was examined as described in Fig. 4. Under conditions allowing nearly equal expression of the Syx5 isoforms and their mutants (Fig. 6A, middle panel), the extent of intracellular  $\beta$ APP accumulation (top panel) in cells expressing Syx5LΔ1-6 or Syx5LΔ1-30 (lanes 3 and 4) was similar to that in cells expressing Syx5L (lane 5). As summarized in Fig. 6B, unlike Syx5 (red bar), neither Syx5LΔ1-6, Syx5LΔ1-30 (gray bars), nor Syx5LA (black bar) were associated with pronounced accumulation of intracellular  $\beta$ APP. Deletion of the di-arginine ER retrieval motif from Syx5L (*i.e.* Syx5LA and Syx5LΔ1-6) partially, but not completely, restored the inhibition of  $\beta$ APP processing (Fig. 6C, black and gray bars). However, there was a trend toward stronger inhibition of A $\beta$ 40 secretion

in the case of the Syx5LΔ1-30 mutant, in which half of the N-terminal extension domain was deleted (Fig. 6C, gray bar). These results suggest that the absence of the whole N-terminal extension may be necessary for the inhibition of  $\beta$ APP processing by Syx5.

**Effect of Overexpression of Syx5 Isoforms on the Processing of  $\beta$ APP in the Presence of ER-to-Golgi Transport Inhibitor, Brefeldin A—**Consistent with observations made in other cells (25), treatment of NG108-15 cells with the fungal toxin brefeldin A (BFA), which strongly inhibits transport from the ER to the Golgi compartments, mimicked Syx5 overexpression by causing marked accumulation of intracellular  $\beta$ APP (Supplementary Fig. S2). When  $\beta$ APP transfected cells were treated with BFA, this accumulation of  $\beta$ APP holoprotein occurred predominantly in the ER. In order to confirm that the two Syx5 isoforms acted differently on  $\beta$ APP metabolism by modulating the trafficking of  $\beta$ APP in the early secretory compartment, we examined the effect of BFA in cells that expressed  $\beta$ APP and were co-transfected with a plasmid that expressed either Syx5 or Syx5L. As shown in Figs 4 and 6, the overexpression of Syx5 in untreated cells (Fig. 7, lane 2 in A, black bars in B and C) caused accumulation of intracellular  $\beta$ APP ( $431.5 \pm 126\%$  of untreated Mock,  $P < 0.001$ ), and reduced the secretion of A $\beta$ 40 ( $37.5 \pm 8.8\%$  of untreated Mock,  $P < 0.001$ ), whereas the overexpression of Syx5L (lane 3 in A, gray bars in B and C) did not. When the cells were treated with BFA, marked accumulation of intracellular  $\beta$ APP holoprotein was observed in all cells (Fig. 7A, top panel, lanes 4–6) regardless of their overexpression of Syx5 isoforms. The levels of intracellular  $\beta$ APP holoprotein in BFA-treated cells that overexpressed Mock, Syx5 or Syx5L were not significantly different (Mock:  $703.1 \pm 280\%$ , Syx5:  $494.8 \pm 202\%$ , Syx5L:  $645.3 \pm 281\%$ , of untreated Mock). Concomitantly, a substantial decrease in A $\beta$ 40 secretion was observed in all cells treated with BFA (Mock:  $19.5 \pm 8.0\%$ , Syx5:  $18.6 \pm 6.1\%$ , Syx5L:  $19.5 \pm 7.8\%$ , of untreated Mock).

## DISCUSSION

Of the syntaxins, which are widely expressed in plant and animal cells, the mammalian syntaxin 5 (Syx5) is

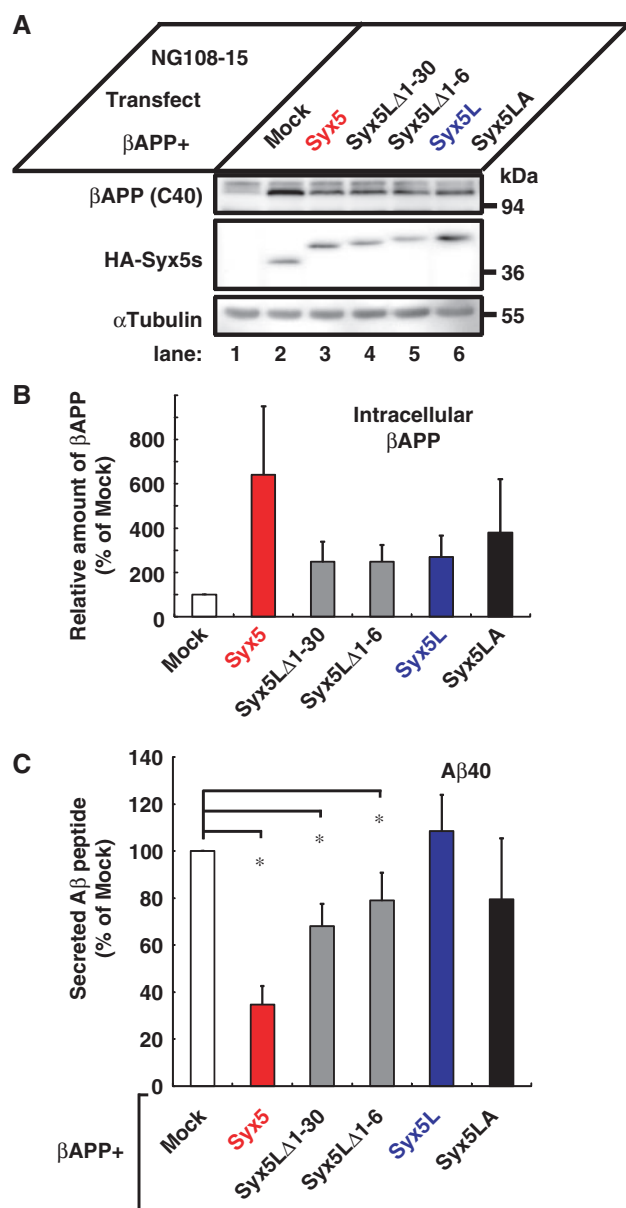


**Fig. 6. Effect of Syx5L mutants on accumulation of intracellular βAPP holoprotein and secretion of Aβ.** (A) NG108-15 cells were co-transfected with plasmids containing the indicated Syx5L mutants along with a cDNA encoding βAPP, and cell extracts were immunoblotted with the indicated antibodies as in Figure 4A. Results shown are representative of seven independent experiments. (B) Intracellular accumulation of βAPP (A, upper panel) was quantified by densitometry. βAPP band intensities were normalized with α-tubulin (A, bottom panel) to give relative amounts and were expressed as a percentage of the control (Mock). Values shown represent the mean ± SD for seven independent experiments. (C) The amount of secreted Aβ40 was quantified as in Figure 4B and is shown as percentage control (Mock). Values shown represent the mean ± SD for 7–19 independent samples. \**P* < 0.01 as determined by Student's *t*-test.

unique in having two isoforms (42 and 35 kDa) that are generated from a single messenger RNA through alternative initiation of translation (7, 10). The longer isoform Syx5L has a putative type-II di-arginine ER-retrieval

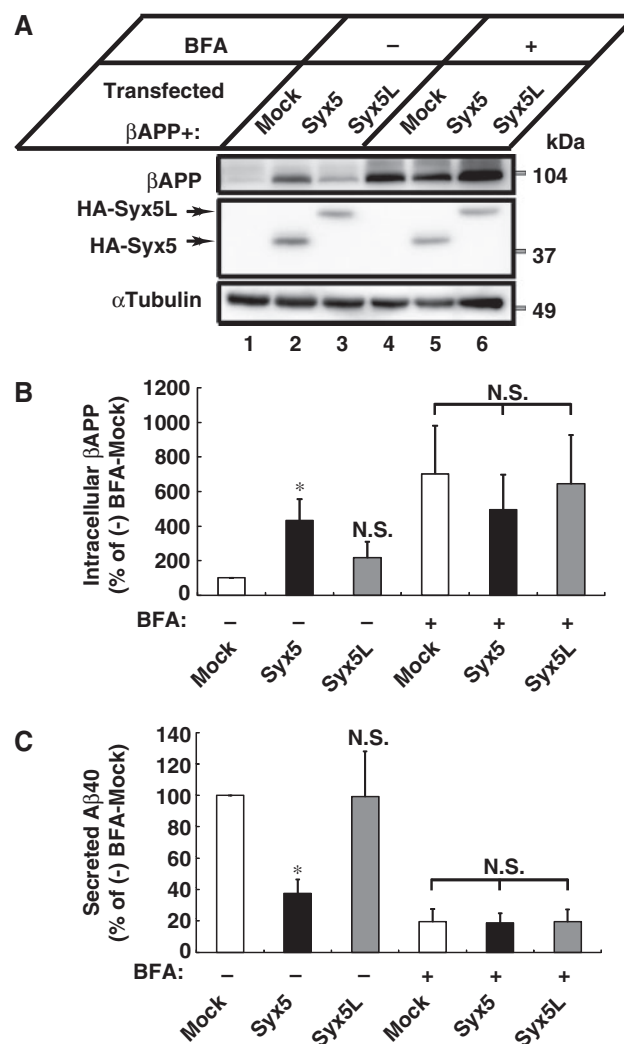


**Fig. 7. Effect of brefeldin A on the processing of βAPP in cells that overexpressed Syx5 isoforms.** (A) NG108-15 cells were co-transfected with the indicated plasmids along with a cDNA encoding βAPP in the absence (–, vehicle, lanes 1–3) or presence (+, 0.2 μg/ml, lanes 4–6) of the ER-to-Golgi transport inhibitor brefeldin A (BFA). Cell extracts prepared 48 h after transfection were subjected to SDS-PAGE and were immunoblotted with the indicated antibodies as in Fig. 6. A representative image is shown. (B) Intracellular accumulation of βAPP holoprotein (A, upper panel) was quantified by densitometry, and the relative amounts βAPP were normalized with α-tubulin (A, bottom panel) and were expressed as a percentage of the control (untreated Mock). Values shown represent the mean ± SD for 11–12 independent samples. \**P* < 0.001 as determined by Student's *t*-test. (C) The amount of secreted Aβ40 from the cells treated with (+) or without (–) BFA was quantified by selective sandwich ELISA, as described in the MATERIALS AND METHODS section, and calculated as a percentage of the control (untreated Mock). Values shown represent the mean ± SD for 11–12 independent samples. \**P* < 0.001 as determined by Student's *t*-test; N.S., not significant.

motif (<sup>4</sup>RKR<sup>6</sup>) in its N-terminal extension region (Fig. 1A). This type of motif near the N-terminus of the extension domain (consensus sequence: RXR) was first identified in the invariant chain of the human major histocompatibility complex class II (26) and was



demonstrated to be sufficient to confer signal activity that localized the protein to the ER (11, 27). In this study, we have shown that this putative motif was functional in NG108-15 cells. This 3-amino-acid motif (RKR) is also present in each subunit of the ATP-sensitive  $K^+$  channel, in which it controls the assembly and trafficking of the  $K^+$  channel complex from the ER to the plasma membrane (28, 29). By analogy with the interaction of the type-I di-lysine motif with  $\alpha$ -COP, one of the coat proteins of the COPI coat (29), the type II di-arginine motif may be recognized by an undefined protein(s), since masking of the signal after formation of the complex of ATP-sensitive  $K^+$  channel subunits allows trafficking to the cell surface (28). Although the mechanism by which this type of motif is recognized is not yet understood, we examined whether Syx5L, which bears an ER-retrieval motif, acts like Syx5 in the interaction and processing of AD-related proteins. We have found that both Syx5 and Syx5L bind to the PS holoprotein, but they have distinct functions in modulating the metabolism and trafficking of  $\beta$ APP in the ER through the Golgi compartments.

**Possible Differences in Mechanism of Syx5 Isoforms in the Metabolism of  $\beta$ APP**—Syx5 overexpression, but not Syx5L, inhibited  $A\beta$  secretion because of the increase in the intracellular accumulation of  $\beta$ APP (Fig. 4). The reduced secretion of  $A\beta$  observed in cells that overexpressed Syx5 was not caused by the decreased expression of  $\beta$ APP holoproteins or by a significant reduction in the total amount of PS1N-terminal fragment (17, 18). Syx5 overexpression significantly suppressed  $A\beta$  secretion when C99 (APP-CTF) was used as the substrate for  $\gamma$ -secretase (18). Unlike Syx5, the Syx5L isoform did not cause inhibition of the secretion of  $A\beta$  derived from C99 in NG108-15 cells (data not shown). These results do not exclude the possibility that Syx5 isoforms affect not only the activities of  $\gamma$ -secretase but also  $\beta$ APP cleavage by  $\beta$ -secretases (BACE1). Considering the fact that Syx5 isoforms distinctly affect the level of APP-CTF (Fig. 4A), Syx5 possibly interferes with  $\beta$ APP transport during its processing and cleavage along the secretory pathway, causing it to accumulate in the early secretory compartment, especially at the ER (18). In contrast, the accumulation of  $\beta$ APP holoprotein in the ER was not observed in cells that overexpressed Syx5L (supplementary Fig. S3). In fact, while cells that overexpressed Syx5L showed marked accumulation of intracellular  $\beta$ APP holoprotein when treated simultaneously with the inhibitor of ER-to-Golgi transport (BFA), treatment of cells that overexpressed Syx5 with BFA did not result in further increase in intracellular  $\beta$ APP holoprotein (Fig. 7). Although Syx5L also interacts with PS1 holoproteins (Fig. 3), it may not interfere with the processes of  $\beta$ APP transport.

The clear difference in the actions of Syx5 and Syx5L on  $\beta$ APP processing was not simply a consequence of their different intracellular localization (Figs 1 and 5). This is supported by the fact that the Syx5LA mutant that lacks the di-arginine ER-retrieval motif did not fully acquire the ability to inhibit  $\beta$ APP processing (Fig. 6) observed with Syx5 (Figs 4 and 6). In further support of this notion, analysis of the intracellular distribution

of  $\beta$ APP by SDG fractionation showed that Syx5LA overexpression did not fully mimic the ability of Syx5 to cause sequestration of  $\beta$ APP in the ER compartment (Supplementary Fig. S3). The observation that sequential deletion of the extension domain from Syx5L gradually increased its inhibitory activity against  $A\beta$  secretion (Fig. 6) suggests that the presence of the N-terminal extension domain of Syx5L may prevent it from inhibiting  $\beta$ APP processing. The PSIPRED secondary structure analysis of Syx5L (<http://bioinf.cs.ucl.ac.uk/psipred/psiform.html>) (30, 31) suggests that the Syx5L extension domain is relatively unstructured, comprising non-helical coils and strands (data not shown). Accordingly, unlocking of an intramolecular interaction between the extension domain of Syx5L and the common Syx5 region might be necessary for the inhibitory action. However, we cannot exclude the possibility that other proteins interacting with this domain may modify the function of Syx5. On the basis of these assumptions, we are currently investigating the precise mechanism responsible for the different effects of Syx5 isoforms on the trafficking and processing of  $\beta$ APP.

**Possible role of Syx5 Isoforms in the Trafficking and Processing of AD-related Proteins**—Many reports have implied that malfunctions in the molecules that participate in the trafficking and sorting of membrane proteins might be involved in the pathogenesis of AD (for a review, please see ref. 32). Because PS and  $\beta$ APP are implicated in various cellular functions and their cellular localizations are critical for the production, clearance, and aggregation of  $A\beta$  (33, 34), PS binding partners that do not form  $\gamma$ -secretase complexes with PS may be equally important for the modulation of  $\beta$ APP metabolism. In the ER through the Golgi compartment, both Syx5 isoforms associated with the PS holoprotein. During the trafficking and processing of  $\beta$ APP, it is likely that Syx5 acts as a negative regulator, whereas the Syx5L isoform does not. In order to investigate the reason for this difference, we attempted to elucidate the interaction between  $\beta$ APP and Syx5 or Syx5L. However, we did not detect any interaction between either of the Syx5 isoforms with  $\beta$ APP or APP-CTF (data not shown). Although the Syx5 isoforms do not bind to  $\beta$ APP, they might affect  $\beta$ APP trafficking by interacting with PS1, because PS1 itself has been shown to mediate the trafficking and sorting of  $\beta$ APP in the ER through the Golgi compartments (35–38).

The Syx5L isoform is only found in mammals and not in yeast cells (6, 7, 10, 39), and this isoform is highly expressed in neuronal cells (19). Considering the differential effects of Syx5 and Syx5L on  $\beta$ APP metabolism, it may be possible that perturbation of Syx5 isoform expression in neuronal cells might cause some changes in  $A\beta$  production in the central nervous system. Accordingly, it will be of special interest to study the levels of expression of Syx5 and Syx5L in the brains of patient with AD. Although, at present, the exact reason for the distinct roles of these two Syx5 isoforms in  $\beta$ APP metabolism remains unknown, appropriate amounts (*i.e.* the balance between the levels of two isoforms) of Syx5s in neuronal cells may be crucial for maintaining the physiologic transport of those proteins.

In conclusion, both Syx5 and Syx5L bind to the PS holoprotein in the ER and Golgi compartments of neuronal cells; however, they modulate the metabolism and trafficking of  $\beta$ APP in distinct ways despite their extensive amino acid sequence identity. Although one previous report has addressed the differences between the two Syx5 isoforms (4), the present study is the first to investigate their distinct cellular functions in the processing and trafficking of AD-related proteins. Because PS and  $\beta$ APP are sorted and processed along the secretory and endocytotic pathways, a defect in the transport machinery would affect the physiologic trafficking of these proteins, thereby affecting the generation and secretion of A $\beta$ . Thus, malfunction or down-regulation of Syx5 isoforms may cause the accumulation of excess A $\beta$  peptides found in late-onset AD. However, further investigation of the differences between these isoforms is needed to address this question.

#### ACKNOWLEDGEMENTS

We thank Masumi Sanada for secretarial assistance.

#### FUNDING

This work was supported in part by a Grant-in-Aid (to K.A.) from the Promotion and Mutual Aid Co-operation Program for private schools in Japan; a Grant-in-Aid for Scientific Research for Young Scientists (B) (16700327 to K.S.) from the Ministry of Education, Culture, Sports, Science, and Technology of Japan; the Japan Society for the Promotion of Science (B) (19300133 to K.A.) and (C) (19500327 to K.S.); and a grant from the Kyorin University School of Medicine to K.S.

#### CONFLICT OF INTEREST

None declared.

#### REFERENCES

- Inoue, A., Obata, K., and Akagawa, K. (1992) Cloning and sequence analysis of cDNA for a neuronal cell membrane antigen, HPC-1. *J. Biol. Chem.* **267**, 10613–10619
- Hong, W. (2005) SNAREs and traffic. *Biochim. Biophys. Acta* **1744**, 120–144
- Kasai, K., Suga, K., Izumi, T., and Akagawa, K. (2008) Syntaxin 8 has two functionally distinct di-leucine-based motifs. *Cell. Mol. Biol. Lett.* **13**, 144–154
- Hay, J.C., Klumperman, J., Oorschot, V., Steegmaier, M., Kuo, C.S., and Scheller, R.H. (1998) Localization, dynamics, and protein interactions reveal distinct roles for ER and Golgi SNAREs. *J. Cell Biol.* **141**, 1489–1502
- Kasai, K. and Akagawa, K. (2001) Roles of the cytoplasmic and transmembrane domains of syntaxins in intracellular localization and trafficking. *J. Cell Sci.* **114**, 3115–3124
- Dascher, C., Matteson, J., and Balch, W.E. (1994) Syntaxin 5 regulates endoplasmic reticulum to Golgi transport. *J. Biol. Chem.* **269**, 29363–29366
- Hay, J.C., Chao, D.S., Kuo, C.S., and Scheller, R.H. (1997) Protein interactions regulating vesicle transport between the endoplasmic reticulum and Golgi apparatus in mammalian cells. *Cell* **89**, 149–158
- Jahn, R., Lang, T., and Südhof, T.C. (2003) Membrane fusion. *Cell* **112**, 519–533
- Volchuk, A., Ravazzola, M., Perrelet, A., Eng, W.S., Di Liberto, M., Varlamov, O., Fukasawa, M., Engel, T., Söllner, T.H., Rothman, J.E., and Orci, L. (2004) Countercurrent distribution of two distinct SNARE complexes mediating transport within the Golgi stack. *Mol. Biol. Cell* **15**, 1506–1518
- Hui, N., Nakamura, N., Sönnichsen, B., Shima, D.T., Nilsson, T., and Warren, G. (1997) An isoform of the Golgi t-SNARE, syntaxin 5, with an endoplasmic reticulum retrieval signal. *Mol. Biol. Cell* **8**, 1777–1787
- Schutze, M.P., Peterson, P.A., and Jackson, M.R. (1994) An N-terminal double-arginine motif maintains type II membrane proteins in the endoplasmic reticulum. *EMBO J.* **13**, 1696–1705
- Selkoe, D.J. (2001) Alzheimer's disease: genes, proteins, and therapy. *Physiol. Rev.* **81**, 741–766
- Dries, D.R. and Yu, G. (2008) Assembly, maturation, and trafficking of the gamma-secretase complex in Alzheimer's disease. *Curr. Alzheimer Res.* **5**, 132–146
- Spasic, D., Tolia, A., Dillen, K., Baert, V., De Strooper, B., Vrijens, S., and Annaert, W. (2006) Presenilin-1 maintains a nine-transmembrane topology throughout the secretory pathway. *J. Biol. Chem.* **281**, 26569–26577
- Kim, J., Kleizen, B., Choy, R., Thinakaran, G., Sisodia, S.S., and Schekman, R.W. (2007) Biogenesis of gamma-secretase early in the secretory pathway. *J. Cell Biol.* **179**, 951–963
- Selivanova, A., Winblad, B., Dantuma, N.P., and Farmery, M.R. (2007) Biogenesis and processing of the amyloid precursor protein in the early secretory pathway. *Biochem. Biophys. Res. Commun.* **357**, 1034–1039
- Suga, K., Tomiyama, T., Mori, H., and Akagawa, K. (2004) Syntaxin 5 interacts with presenilin holoproteins, but not with their N- or C-terminal fragments, and affects beta amyloid peptide production. *Biochem. J.* **381**, 619–628
- Suga, K., Saito, A., Tomiyama, T., Mori, H., and Akagawa, K. (2005a) Syntaxin5 interacts specifically with presenilin holoproteins and affects processing of betaAPP in neuronal cells. *J. Neurochem.* **94**, 425–439
- Suga, K., Hattori, H., Saito, A., and Akagawa, K. (2005b) RNA interference-mediated silencing of the syntaxin 5 gene induces Golgi fragmentation but capable of transporting vesicles. *FEBS Lett.* **579**, 4226–4234
- Suga, K., Yamamori, T., and Akagawa, K. (2003) Identification of the carboxyl-terminal membrane-anchoring region of HPC-1/Syntaxin 1A with the substituted-cysteine-accessibility method and monoclonal antibodies. *J. Biochem.* **133**, 325–334
- Bradford, M.M. (1976) A rapid and sensitive method for the quantitation of microgram quantities of protein utilizing the principle of protein-dye binding. *Anal. Biochem.* **72**, 248–254
- Laemmli, U.K. (1970) Cleavage of structural proteins during the assembly of the head of bacteriophage T4. *Nature* **227**, 680–685
- Schägger, H. and von Jagow, G. (1987) Tricine-sodium dodecyl sulfate-polyacrylamide gel electrophoresis for the separation of proteins in the range from 1 to 100 kDa. *Anal. Biochem.* **166**, 368–379
- Greenfield, J.P., Tsai, J., Gouras, G.K., Hai, B., Thinakaran, G., Checler, F., Sisodia, S.S., Greengard, P., and Xu, H. (1999) Endoplasmic reticulum and trans-Golgi network generate distinct populations of Alzheimer beta-amyloid peptides. *Proc. Natl Acad. Sci. USA* **96**, 742–747
- Grimm, H.S., Beher, D., Lichtenthaler, S.F., Shearman, M.S., Beyreuther, K., and Hartmann, T. (2003) gamma-secretase cleavage site specificity differs for intracellular and secretory amyloid beta. *J. Biol. Chem.* **278**, 13077–13085
- Strubin, M., Mach, B., and Long, E. O. (1984) The complete sequence of the mRNA for the HLA-DR-associated invariant chain reveals a polypeptide with an unusual transmembrane polarity. *EMBO J.* **3**, 869–872

27. Lotteau, V., Teyton, L., Peleraux, A., Nilsson, T., Karlsson, L., Schmid, S.L., Quaranta, V., and Peterson, P.A. (1990) Intracellular transport of class II MHC molecules directed by invariant chain. *Nature* **348**, 600–605
28. Zerangue, N., Schwappach, B., Jan, Y.N., and Jan, L.Y. (1999) A new ER trafficking signal regulates the subunit stoichiometry of plasma membrane K(ATP) channels. *Neuron* **22**, 537–548
29. Zerangue, N., Malan, M.J., Fried, S.R., Dazin, P.F., Jan, Y.N., Jan, L.Y., and Schwappach, B. (2001) Analysis of endoplasmic reticulum trafficking signals by combinatorial screening in mammalian cells. *Proc. Natl Acad. Sci. USA* **98**, 2431–2436
30. Jones, D.T. (1999) Protein secondary structure prediction based on position-specific scoring matrices. *J. Mol. Biol.* **292**, 195–202
31. McGuffin, L.J., Bryson, K., and Jones, D.T. (2000) The PSIPRED protein structure prediction server. *Bioinformatics* **16**, 404–405
32. Small, S.A. and Gandy, S. (2006) Sorting through the cell biology of Alzheimer's disease: intracellular pathways to pathogenesis. *Neuron* **52**, 15–31
33. Huse, J.T., Liu, K., Pijak, D.S., Carlin, D., Lee, V.M., and Doms, R.W. (2002) Beta-secretase processing in the trans-Golgi network preferentially generates truncated amyloid species that accumulate in Alzheimer's disease brain. *J. Biol. Chem.* **277**, 16278–16284
34. Lee, E.B., Zhang, B., Liu, K., Greenbaum, E.A., Doms, R.W., Trojanowski, J.Q., and Lee, V.M. (2005) BACE overexpression alters the subcellular processing of APP and inhibits Abeta deposition in vivo. *J. Cell Biol.* **168**, 291–302
35. Naruse, S., Thinakaran, G., Luo, J.J., Kusiak, J.W., Tomita, T., Iwatsubo, T., Qian, X., Ginty, D.D., Price, D.L., Borchelt, D.R., Wong, P.C., and Sisodia, S.S. (1998) Effects of PS1 deficiency on membrane protein trafficking in neurons. *Neuron* **21**, 1213–1221
36. Cai, D., Leem, J.Y., Greenfield, J.P., Wang, P., Kim, B.S., Wang, R., Lopes, K.O., Kim, S.H., Zheng, H., Greengard, P., Sisodia, S.S., Thinakaran, G., and Xu, H. (2003) Presenilin-1 regulates intracellular trafficking and cell surface delivery of beta-amyloid precursor protein. *J. Biol. Chem.* **278**, 3446–3454
37. Réchards, M., Xia, W., Oorschot, V., van Dijk, S., Annaert, W., Selkoe, D.J., and Klumperman, J. (2006) Presenilin-1-mediated Retention of APP Derivatives in Early Biosynthetic Compartments. *Traffic* **7**, 354–364
38. Gandy, S., Zhang, Y.W., Ikin, A., Schmidt, S.D., Bogush, A., Levy, E., Sheffield, R., Nixon, R.A., Liao, F.F., Mathews, P.M., Xu, H., and Ehrlich, M. E. (2007) Alzheimer's presenilin 1 modulates sorting of APP and its carboxyl-terminal fragments in cerebral neurons in vivo. *J. Neurochem.* **102**, 619–626
39. Hardwick, K.G. and Pelham, H.R. (1992) SED5 encodes a 39-kD integral membrane protein required for vesicular transport between the ER and the Golgi complex. *J. Cell Biol.* **119**, 513–521